JVI Journals.ASM.org

Canine Distemper Virus Envelope Protein Interactions Modulated by Hydrophobic Residues in the Fusion Protein Globular Head

Mislay Avila,[a,b] Mojtaba Khosravi,[a,b] Lisa Alves,[a,b] Nadine Ader-Ebert,[a,b] Fanny Bringolf,[a,b] Andreas Zurbriggen,[a] Richard K. Plemper,[c] Philippe Plattet[a]

Division of Neurological Sciences, DCR-VPH, Vetsuisse Faculty, University of Bern, Bern, Switzerland[a]; Graduate School for Cellular and Biomedical Sciences, University of Bern, Bern, Switzerland[b]; Institute for Biomedical Sciences, Georgia State University, Atlanta, Georgia, USA[c]

Membrane fusion for morbillivirus cell entry relies on critical interactions between the viral fusion (F) and attachment (H) envelope glycoproteins. Through extensive mutagenesis of an F cavity recently proposed to contribute to F's interaction with the H protein, we identified two neighboring hydrophobic residues responsible for severe F-to-H binding and fusion-triggering deficiencies when they were mutated in combination. Since both residues reside on one side of the F cavity, the data suggest that H binds the F globular head domain sideways.

Measles virus (MeV) and canine distemper virus (CDV) belong to the *Morbillivirus* genus of the *Paramyxovirus* family. MeV remains responsible for major human mortality, with approximately 120,000 measles-associated deaths per year (1), and CDV exhibits an ever-increasing host range in wild aquatic and terrestrial carnivores, often with devastating consequences (2–4).

The MeV and CDV cell entry systems depend on two interacting surface glycoproteins: the tetrameric receptor-binding H protein and the trimeric F protein (5). In the first step, the H protein binds to cell surface receptors (SLAM or nectin-4, depending on the type of target cells) through its membrane-distal cuboidal head domain (6–10). It is thought that receptor engagement then leads to opening of the central section of the H stalk through putative H head movements (11–13), which in turn actively destabilize prefusion F complexes (14, 15). Destabilized F trimers then undergo irreversible conformational changes that eventually lead to membrane merger and fusion pore formation (5, 16).

Proper assembly of the H-F glycoprotein complexes is therefore critical for membrane fusion triggering and is believed to occur early within the host secretory pathway (17). A region spanning residues 111 to 118 in the H stalk domain was proposed as a candidate microdomain mediating F-H interaction (11, 18, 19). More recently, several candidate residues in F were postulated to engage in short-range interactions with H. Indeed, key substitutions near the fusion peptide or at the base of the F trimer led to a significant reduction in bioactivity, but this phenotype correlated only with moderate impairments of physical glycoprotein interactions (18, 20).

In this study, we therefore aimed at generating fusion-defective F mutants retaining proper folding into the prefusion conformation, proteolytic processing, and cell surface transport but exhibiting severe deficiencies in H-binding activity. We conducted a systematic mutagenesis analysis of the region located at the base of the CDV F trimer head, which is homologous to the MeV F microdomain that was recently proposed to interact with the MeV H stalk (20). Interestingly, the targeted microdomain defines a large cavity that is formed by two adjacent F monomers (Table 1 and Fig. 1A). In a first round of mutagenesis, a total of 29 residues were mutated to alanine (the alanine residue at position 279 was changed to serine); 17 of these were predicted to be located in one of the monomers lining the cavity, and 12 were predicted in the other (Table 1 and Fig. 1A).

The resulting panel of F variants was initially screened for fusion activity using a well-established transient cell-to-cell fusion assay and Vero-SLAM cells. Ten out of the 29 single F mutants were clearly impaired in fusion activity, consistent with data obtained previously for MeV F trimers (20). Of those, six showed strong fusion defects while remaining efficiently surface expressed in their prefusion conformation (E422A, Y436A, L437A, L482A, L506A, and K508A) (Table 1 and Fig. 1B). Of note, we used the recently described prefusion and postfusion conformation-specific monoclonal anti-CDV-F antibodies (MAbs) (4941 and 4068, respectively [14]) to probe the conformational change of each F mutant. All F proteins carried, in addition, a FLAG epitope tag in the ectodomain, which we have previously shown not to significantly modulate bioactivity (14). Cell surface expression was quantified using a monoclonal anti-FLAG antibody and flow cytometry after immunostaining.

Hydrophobic-protein-protein interfaces were recently proposed as major contributing factors regulating paramyxovirus envelope protein interaction (20, 21), and indeed, the cavity microdomain of CDV F contains a considerable number of hydrophobic residues that are predicted to be solvent exposed by our CDV F structural model (22). To specifically test a role of hydrophobic contacts in H-F interaction, we made, in a second round of mutagenesis, hydrophobic-to-polar or charged substitutions at four of the six critical F cavity positions (two mutations

Received 23 June 2014 **Accepted** 26 October 2014

Accepted manuscript posted online 29 October 2014

Citation Avila M, Khosravi M, Alves L, Ader-Ebert N, Bringolf F, Zurbriggen A, Plemper RK, Plattet P. 2015. Canine distemper virus envelope protein interactions modulated by hydrophobic residues in the fusion protein globular head. J Virol 89:1445–1451. doi:10.1128/JVI.01828-14.

Editor: A. García-Sastre

Address correspondence to Philippe Plattet, philippe.plattet@vetsuisse.unibe.ch.

M.A. and M.K. contributed equally to this article.

doi:10.1128/JVI.01828-14

TABLE 1 Summary of properties of 29 single-alanine F mutants[a]

Mutation	Monomer	FA	CSE	Conf (37°C)
None (wt)	–	4+	100.0 ± 0.0	Pre
I157A	A	0	53.0 ± 7.8	Pre
T159A	A	4+	94.5 ± 17.0	Pre
R160A	A	4+	95.8 ± 8.4	Pre
A279S	A	4+	103.9 ± 9.6	Pre
T280A	A	4+	99.0 ± 19.9	Pre
Q281A	A	4+	107.4 ± 19.4	Pre
V403A	A	4+	86.4 ± 6.4	Pre
K404A	A	4+	90.9 ± 7.4	Pre
G405A	A	4+	33.9 ± 11.9	Pre
S420A	B	4+	97.0 ± 17.8	Pre
Q421A	B	4+	96.3 ± 9.4	Pre
E422A	B	2+	81.2 ± 44.3	Pre
N434A	A	4+	62.2 ± 13.5	Pre
Y436A	A	2+	76.5 ± 6.8	Pre
L437A	A	1+	73.5 ± 8.7	Pre
S439A	A	4+	89.1 ± 19.3	Pre
Q457A	A	4+	101.0 ± 13.1	Pre
N458A	A	4+	89.2 ± 23.6	Pre
L460A	A	4+	50.4 ± 9.5	Pre
P462A	A	4+	93.0 ± 11.5	Pre
L482A	B	2+	77.1 ± 29.2	Pre
S484A	B	3+	105.1 ± 12.4	Pre
G485A	B	3+	101.2 ± 20.8	Pre
T486A	B	4+	101.7 ± 9.5	Pre
S504A	B	4+	97.0 ± 16.0	Pre
I505A	B	0	58.5 ± 7.0	Pre/post
L506A	B	1+	78.6 ± 41.6	Pre
K508A	B	1+	66.6 ± 15.0	Pre
D538A	B	3+	90.7 ± 18.6	Pre

[a] Mutations indicate the positions of alanine substitutions (except alanine at position 279, which was mutated into a serine). The monomer is the F monomer in which the mutation occurs, defining one cavity of the trimer. Fusion activity (FA) was monitored by a transient F/H-induced cell-cell fusion assay. A fusion score was attributed to the standard and mutated F proteins as follows: 0, no fusion; 1+, limited fusion; 2+, moderate fusion; 3+, strong fusion; and 4+, massive fusion. Cell surface expression (CSE) was monitored by immunofluorescence (anti-FLAG staining) followed by flow cytometry (normalized to that of F-wt). The conformational state of F at 37°C (Conf 37°C) was assessed with previously reported conformation-sensitive MAbs (Pre, prefusion-F-recognizing MAb, and post, postfusion-F-recognizing MAb). "–," not applicable.

were introduced into each of the two monomers that define one cavity), resulting in F variants F-L437D or F-L437Q, F-L482D or F-L482Q, F-L506D or F-L506Q, and F-K508E or F-K508R (Table 2). Strikingly, cell-to-cell fusion assays revealed that all mutants were either completely or nearly completely defective in membrane fusion triggering (Table 2 and Fig. 1C). Importantly, with the F conformation-sensitive MAbs, immunofluorescence staining followed by flow cytometry analyses revealed that the eight newly designed F mutants preserved their prefusion conformational state (Table 2). In addition, with the anti-FLAG MAb, flow cytometry data indicated that all proteins were properly transported to the cell surface, although F-L482D exhibited some deficiency (Table 2).

To investigate whether impaired triggering of F refolding correlated with physical disengagement of the mutant F trimers from the H protein, coimmunoprecipitation (coIP) experiments were conducted. Using a semiquantitative cell surface H/F coIP assay initially developed by Paal and colleagues (19), we noted that F mutants F-L506D, -L506Q, -K508E, and -K508R were impaired in H binding (their coIP efficiencies were approximately 40 to 60% of that of wild-type F [F-wt]) (Fig. 2A and B). Western blot analysis of total F protein clearly indicated that all F_0 precursors were properly processed. The only exception was mutant F-L482D (Fig. 2A, TL blots). We also noted that some mutants displayed slight mobility shifts of their F_0 and F_1 subunits. Since proteins were separated by SDS-PAGE under reducing conditions, these shifts most likely resulted from the alteration of the hydrophobic nature of the selected residues into charged or polar amino acids (Fig. 2A).

Since both the F-L506D and F-K508E mutations led to fusion deficiency and had a moderate effect on H binding, we speculated that combining both substitutions might lead to a more severe phenotype (Fig. 3A). Thus, in a third round of mutagenesis, the double F variant (F-L506D/K508E) was engineered and its ability to induce membrane fusion investigated in cell-to-cell fusion assays. As anticipated, F-L506D/K508E was completely fusion defective (Fig. 3B). Biochemical characterization reveled that substitutions of both hydrophobic residues into charged amino acids resulted in slightly impaired folding and processing activities; reduced values compared to that for F-wt were recorded for both cell surface expression and F_0 maturation efficiency (Fig. 3C and Table 2). Because of this reduction in surface expression of the double F mutant compared to that of F-wt, we also assessed the intrinsic stability of mutant prefusion F complexes. Indeed, we recently demonstrated that the height of the activation energy barrier modulates the fusion activity of morbillivirus F trimers (14, 15). We therefore determined the temperature at which the trimers changed conformations using both F conformation-sensitive MAbs (for comparison, F-wt and the F-K508E variant were also included in this assay). The temperature at which 50% of the F population was present in the pre- and postfusion states served as an indicator of the intrinsic stability of the selected F protein. Importantly, results summarized in Table 2 indicate that the F-K508E and F-L506D/K508E mutants maintained wt-like prefusion intrinsic F stability (Table 2), despite the slight reduction in cell surface expression of the double F mutant. Strikingly, coIP experiments revealed that F-L506D/K508E was drastically impaired in H binding, with an avidity of interaction of less than 20% of that recorded for H-wt with F-wt. Taking these findings together, we observed an additive effect of two neighboring substitutions located in one face of the F cavity microdomain.

Despite recent progress in our structural and mechanistic understanding of the paramyxovirus cell entry process (reviewed in references 23 to 25), precisely how paramyxovirus envelope proteins assemble prior to receptor engagement remains to be elucidated. To shed light on the morbillivirus glycoproteins' interaction cascade, we aimed in this study to design "fusion-dead" CDV F mutants as a result solely of the physical separation of the F and H proteins, despite proper overall F folding, proteolytic processing, and cell surface transport competence. Toward this goal, we performed a thorough mutagenesis analysis of a cavity F microdomain located near the bottom of the globular head domain. Two recent reports suggested that this large pocket (or part of it) contributes to controlling the physical interaction of F with the attachment protein (20, 21). Interestingly, this cavity is defined by the apposition of two adjacent monomers and is predicted to contain a considerable number of solvent-exposed hydrophobic amino acids, which may create a hydrophobic interface available for interaction with H. Consistently with previous results (20), single alanine substitutions at key positions in the cavity influ-

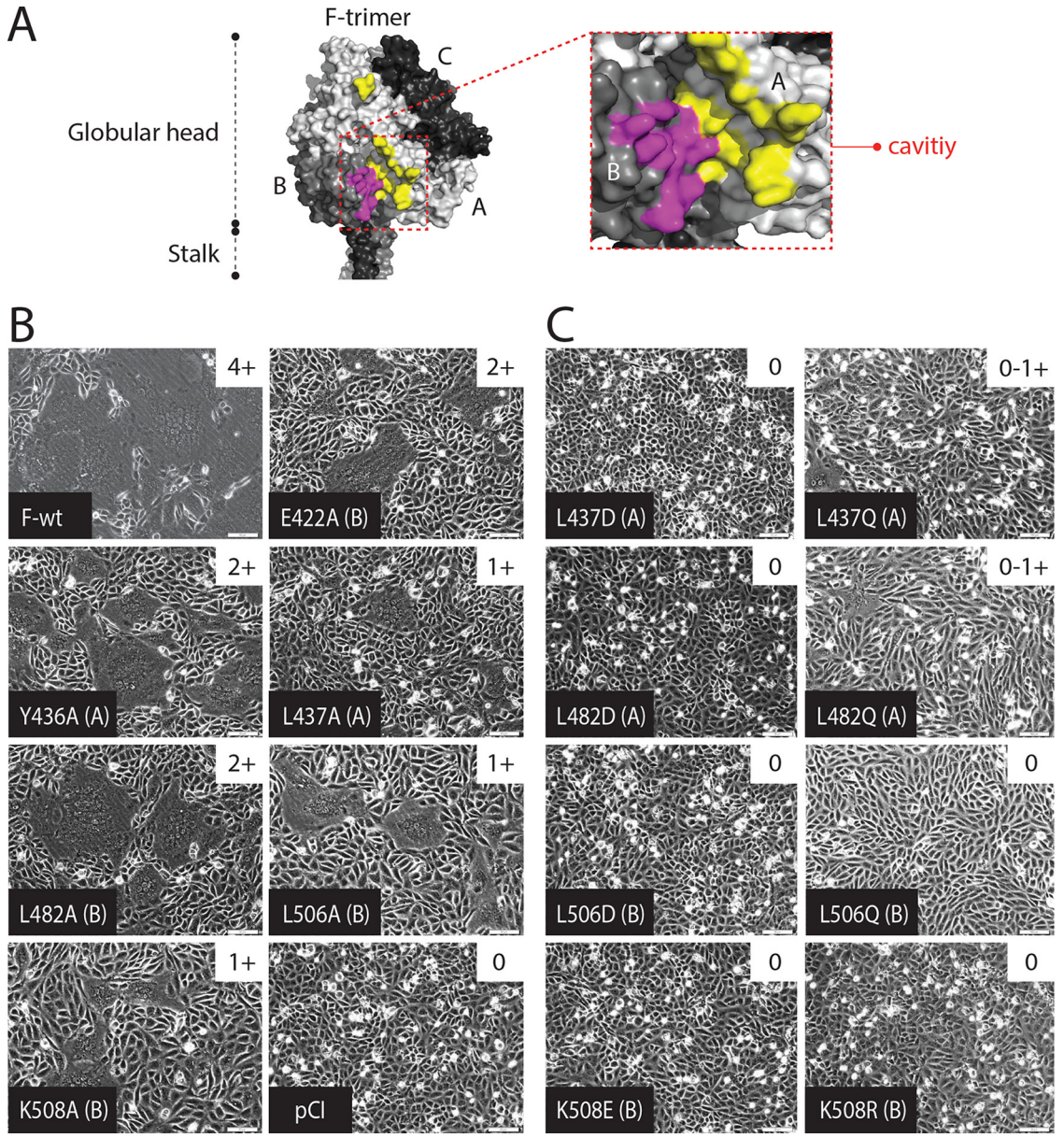

FIG 1 Identification of residues influencing the physical interaction of H and F. (A) Homology model of the prefusion CDV F trimer. Residues defining the cavity of the F trimer that were mutated to alanine are color coded. For the presented cavity, residues in yellow are present in monomer A, whereas residues in violet are present in monomer B. (B and C) Syncytium formation assay. Cell-to-cell fusion activities triggered by coexpression of CDV H and CDV F (A75/17 strain) or CDV H and various CDV F mutants in Vero cells expressing the SLAM receptor. Upper right insets contain fusion scores. Fusion was scored as follows: 0, no fusion; 1+, limited fusion; 2+, moderate fusion; 3+, strong fusion; and 4+, massive fusion. The monomer (defining one cavity of the F trimer) where the mutation occurs is indicated in parentheses.

enced the H-F interaction, albeit only to a limited extent. In sharp contrast, multiple polar or charged amino acid substitutions in the cavity at residues L506 and K508 created an F mutant with the desired phenotype: strongly impaired in fusion and H-binding activities but lacking a significant defect in folding, processing, and cell surface transport competence.

It has been proposed that residues located in the H stalk section (residues 110 to 118) are involved in a short-range interaction with F trimers (18) and that tetrameric H stalks may assume a 4-helix bundle (4HB) conformation prior to receptor binding (11–13). Moreover, it is noteworthy that in our structural model of prefusion CDV F, residues L506 and K508 were located on one side of the cavity (which assumes an Ig-like conformation) and toward the rim of the pocket (Fig. 3A). Hence, these predictions support a model in which the compact 4HB H stalk domain may engage in short-range interactions with the Ig-like domain of the F globular head domain. This model is consistent with recent findings obtained for parainfluenza virus type 5 (PIV5) hemagglutinin-neuraminidase (HN)–F interactions (21), but it interestingly slightly differs from a hypothesis recently put forward for measles virus, which predicted that H stalks might dock directly into the F cavity microdomain (20).

TABLE 2 Summary of properties of nine F proteins with polar or charged substitutions at critical positions[a]

Mutation(s)	Monomer	FA	CSE	TCS (°C)
None (wt)	–	4+	100.0 ± 0.00	60–62
L437D	A	0	99.2 ± 21.2	ND
L437Q	A	0–1+	98.1 ± 4.6	ND
L482D	B	0	56.2 ± 9.4	ND
L482Q	B	0–1+	93.4 ± 7.0	ND
L506D	B	0	126.7 ± 27.5	ND
L506Q	B	0	114.3 ± 21.1	ND
K508E	B	0	89.9 ± 17.5	60–62
K508R	B	0	101.8 ± 24.6	ND
L506D K508E	B/B	0	61.1 ± 7.7	60–62

[a] Mutations indicate the positions of the substitutions. The monomer is the F monomer in which the mutation occurs, defining one cavity of the trimer. Fusion activity (FA) was monitored by a transient F/H-induced cell-cell fusion assay. A fusion score was attributed to the standard and mutated F proteins as follows: 0, no fusion; 1+, limited fusion; 2+, moderate fusion; 3+, strong fusion; and 4+, massive fusion. Cell surface expression (CSE) was monitored by immunofluorescence (anti-FLAG staining) followed by flow cytometry (normalized to that of F-wt). The conformational state of F at 37°C was assessed with previously reported conformation-sensitive MAbs; in all cases, the MAb recognized prefusion F. The temperature of conformational switching (TCS) is the temperature at which F trimers switch conformation from the prefusion to the postfusion state (assessed by immunofluorescence [IF] and flow cytometry with previously described conformation-sensitive anti-F monoclonal antibodies). ND, not determined; "–," not applicable.

Importantly, MeV and PIV5 F residues analogous to CDV F leucine 506 (L394 and L384, respectively) are conserved and were also suggested to be involved in short-range interactions with the respective attachment proteins (20, 21). In contrast, residue L325 (residing on the opposite face of the cavity) was shown only in MeV F to impact the interaction with H; indeed, the analogous conserved residues F-L315 in PIV5 and F-L437 in CDV had no significant impact on the glycoprotein interactions (20, 21). For PIV5 F, additional residues present on the Ig-like side of the F cavity were proposed to be involved in short-range interactions with PIV5 HN, but all residues probed on the opposite side of the pocket reportedly did not influence the HN-F interaction (21). Interestingly, adaptation of human parainfluenza virus type 3 to grow in airway epithelium led to one mutation in the Ig-like domain of the F globular head domain that indeed led to the modulation of cell-to-cell fusion activity (26). Overall, while these data may indicate subtle differences in how glycoproteins interact among different paramyxoviruses, the Ig-like domain (one side of the cavity) seems to be systemically involved.

Based on previous findings, either an inverse (27–29) or a direct (30) correlation was suggested between attachment protein and F avidity of interactions and fusion triggering efficiency, two phenotypes that appeared to correlate with attachment proteins interacting with proteinaceous or sialic acid-containing receptors, respectively (reviewed in references 31 and 32). We propose that decreasing the avidity of attachment protein-F interactions initially leads to increased fusion activity, but there is obviously a reasonable limit, and overcoming this threshold, resulting in a lack of any appreciable interaction, then switches to fusion impairments. Alternatively, mutations that reportedly modulate the strength of glycoprotein interactions may impact bioactivity through other, more-indirect molecular mechanisms (i.e., the intrinsic F-triggering capacity of the H protein or the inherent ability of F to refold from pre- to postfusion structures).

Does the proposed attachment protein stalk-F head interaction represent the initial binding mode of the glycoproteins? Although two discrete tetrameric conformations of MeV H heads were crystallized (33), the atomic coordinates of the morbillivirus H stalk domains remain to be determined. Interestingly, both H head configurations contrast with two recently determined structures of the related parainfluenza virus type 5 (PIV5) (34) and Newcastle disease virus (NDV) HN ectodomains (35). While the NDV HN structure revealed two dimeric head units backfolding on ei-

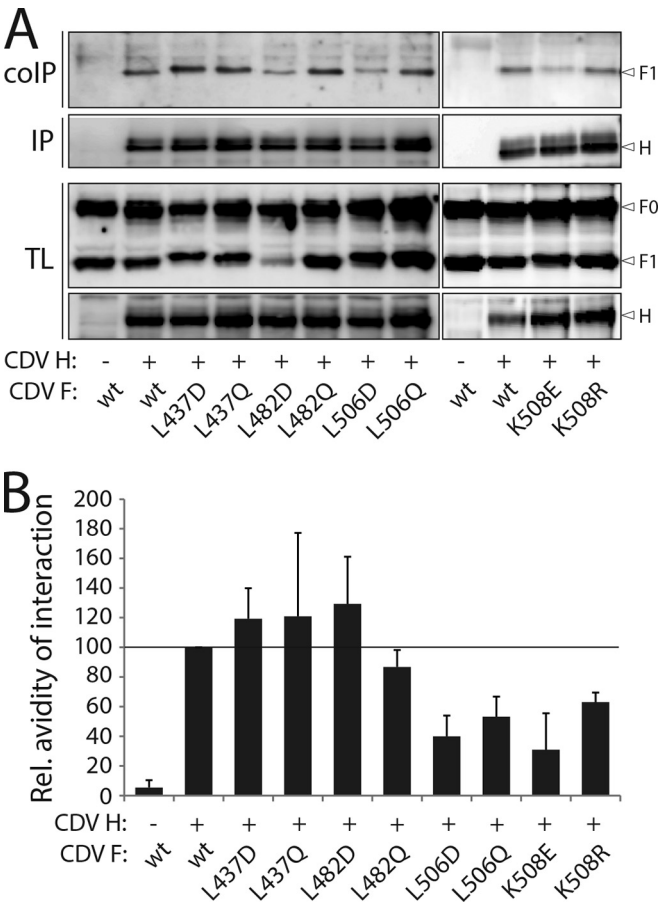

FIG 2 Substitution of critical hydrophobic residues in F with polar or charged amino acids impaired H binding activity. (A) Cell surface assessment of H interaction with cleaved F proteins. To stabilize H-F complexes, transfected Vero cells were treated with the non-membrane-permeable cross-linker dithiobis(sulfosuccinimidylpropionate) (DTSSP) and subsequently lysed with radioimmunoprecipitation assay (RIPA) buffer. Complexes were then immunoprecipitated (IP) with anti-CDV H MAbs 2267 and 3734 (40) and protein G-Sepharose bead treatment. Proteins were boiled and subjected to immunoblotting using a polyclonal anti-CDV-F antibody (41) to detect F antigenic materials (coIP). CoIP F proteins were detected in comparison with F proteins present in cell lysates prior to IP by immunoblotting using the same anti-F antibody (TL, total lysate; F_0, uncleaved F protein; F_1, cleaved membrane-anchored F subunit). (B) Semiquantitative assessment of F/H avidity of interactions. To quantify the avidities of F_1-H interactions, the signals in each F_1 and H band were quantified using the AIDA software package. The avidity of F_1-H interactions is represented by the ratio of the amount of coimmunoprecipitated (coIP) F_1 over the product of F_1 in the cell lysates divided by the ratio of the amount of immunoprecipitated H over the product of H in the cell lysate [(coIP F_1/TL F_1)/(IP H/TL H)]. Subsequently, all ratios were normalized to the ratio of the wild-type F-H interactions, set to 100%. Values are averages of results from at least three independent experiments.

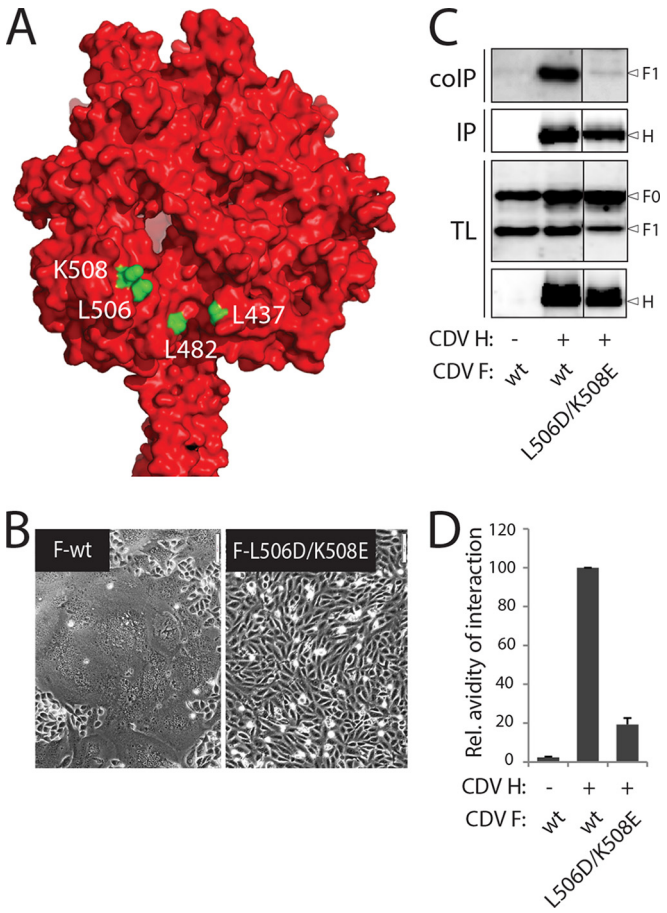

FIG 3 Additive effect on H-F glycoprotein interaction by combined mutations in CDV F. (A) Homology model of the prefusion CDV F trimer (red). The four critical residues in the cavity F microdomain that dramatically affected membrane fusion when they were changed to polar or charged amino acids are highlighted in green. (B) Syncytium formation assay. Cell-to-cell fusion activity was determined as described in the legend to Fig. 1B. (C) Cell surface assessment of H interaction with cleaved F proteins. CoIPs were performed as described in the legend to Fig. 2A. For clarity, gels were cropped, and the black lines indicate the cropping site. (D) Semiquantitative assessment of F/H avidity of interactions. The strength of F-H interactions was calculated as described in the legend to Fig. 2B. Values are averages of results from at least three independent experiments.

ther side of the 4HB stalk (referred to as the "four heads down" conformation), the most recent atomic structure of PIV5 HN was characterized by one dimeric head unit assuming a "down" configuration and the other one folded in a "heads up" state with a helix extending beyond the 4HB stalk domain (referred to as the "two heads down and two heads up" conformation). Importantly, a PIV5 HN four heads down conformation implies that the two lower heads interact with the C-terminal part of the stalk domain, which carries the putative F activation/binding sites. Hence, intracellular HN stalk-F functional interaction is prevented and would occur only after receptor binding by HN, when the HN heads are proposed to move in the "up" state and unmask the critical F-activating/binding sites (referred to as the "stalk exposure" model [24, 34, 36]). Consequently, the HN stalk-F head physical contact was proposed to trigger an "induced-fit" mechanism that ultimately leads to F refolding (36).

In contrast, intracellular association of H/F hetero-oligomer complexes has been described in the case of morbilliviruses (17). While MeV and CDV H proteins may also assume a "four heads down"-like configuration, we hypothesize that due to longer stalk sequences, H heads may interact with the C-terminal region of the stalk without covering the F-binding sites. Consequently, the H stalk section from positions 110 to 118 may be able to dock onto the Ig-like domain of F trimers while the complexes are still in the endoplasmic reticulum (ER) of the host cell, as demonstrated for MeV glycoproteins (17). Alternatively, H proteins may assume a "two heads up and two heads down"-like conformational state that could support intracellular H-F assembly via the single exposed F docking site. While it will be very informative to experimentally test these alternatives, we propose that in either case intracellular morbillivirus H-F contacts remain nonproductive, even after F_0 proteolytic processing in the Golgi apparatus, until H binds to its receptor on a target cell membrane.

Interestingly, among others, a new model has recently been proposed by Liu and colleagues (37). In this model, the F protein of Nipah virus (NiV) initially binds to the attachment protein (G) head domains before switching to the stalks as a consequence of receptor binding. Although a receptor-induced sequential F-to-G binding mechanism may exist in NiV, results obtained with morbilliviruses are not directly compatible with this model. Indeed, mutations in both the MeV and CDV H stalks (residues 110 to 114) led to a significant reduction in F-binding ability even in the absence of receptor engagement (12, 19, 38). Thus, future studies are required to validate or reject these different models of membrane fusion triggering.

How can morbillivirus H/receptor binding trigger the F refolding cascade? We and others have demonstrated that the central section of the morbillivirus H stalk domain undergoes a conformational change upon H/receptor engagement leading to F triggering (11–13). Since it has recently been reported that MeV H proteins lacking the head domains remain bioactive (if properly stabilized [39]), H heads may undergo a conformational change that might result in "unclamping" of the stalks, which then may spontaneously refold into the open-stalk F-triggering conformation. Receptor-induced opening of the central stalk section may then first translate into H/F dissociation, thereby unmasking (and hence exposing to solvent) the previously covered critical hydrophobic residues. Such signals may then extend to the nearby central pocket microdomain that was recently shown to contribute to the regulation of the stability of prefusion F complexes (15) and may eventually result in complete destabilization of prefusion F trimers and release of the fusion peptides.

F trimers expressed in the absence of H reach the cell surface in prefusion conformation. The lack of the proposed cavity-uncovering event may be the reason why these F trimers do not spontaneously refold despite permanently exposed hydrophobic residues in the cavity domains. The precise H-to-F stoichiometry in functional fusion complexes is not known. However, we consider it most likely that induced exposure of only one Ig-like domain to solvent is sufficient to trigger the conformational changes. Interestingly, substitution of only one of the two key regulating residues (L506 and K508) was sufficient to drastically modulate membrane fusion activity, whereas a combination of mutations was required to substantially reduce the physical interaction with H. In addition, a single substitution at the opposite side of the pocket (L437) also strongly abrogated membrane fusion activity, although it did not significantly influence H-F interactions. These

data suggest that the Ig-like domain of the pocket may be involved in a short-range interaction with H, but the cavity in its entirety is required to receive and further conduct the signal, ultimately leading to destabilization and refolding of the F trimer, as was recently suggested for MeV F (20). Further studies are needed to unravel the exact changes that may occur at the glycoprotein-glycoprotein interface at the time of fusion triggering.

Taken together, our findings demonstrate that two hydrophobic residues located in the Ig-like domain of the F globular head domain very likely contribute to physical interaction with the membrane-proximal domain of the H stalk. These data advance our mechanistic insight into paramyxovirus glycoprotein interaction and shed important new light on our general understanding of the paramyxovirus cell entry system.

ACKNOWLEDGMENTS

This work was supported by the Swiss National Science Foundation (reference no. 310030_153281 to P.P.), by the Novartis Foundation for Biomedical Research (reference no. 14A08 to P.P.), and, in part, by Public Health Service grants AI083402 and AI071002 from the NIH/NIAID (to R.K.P.).

REFERENCES

1. **Chen SY, Anderson S, Kutty PK, Lugo F, McDonald M, Rota PA, Ortega-Sanchez IR, Komatsu K, Armstrong GL, Sunenshine R, Seward JF.** 2011. Health care-associated measles outbreak in the United States after an importation: challenges and economic impact. J Infect Dis **203:** 1517–1525. http://dx.doi.org/10.1093/infdis/jir115.
2. **Sakai K, Nagata N, Ami Y, Seki F, Suzaki Y, Iwata-Yoshikawa N, Suzuki T, Fukushi S, Mizutani T, Yoshikawa T, Otsuki N, Kurane I, Komase K, Yamaguchi R, Hasegawa H, Saijo M, Takeda M, Morikawa S.** 2013. Lethal canine distemper virus outbreak in cynomolgus monkeys in Japan in 2008. J Virol **87:**1105–1114. http://dx.doi.org/10.1128/JVI.02419-12.
3. **Roelke-Parker ME, Munson L, Packer C, Kock R, Cleaveland S, Carpenter M, O'Brien SJ, Pospischil A, Hofmann-Lehmann R, Lutz H, Mwamengele GL, Mgasa MN, Machange GA, Summers BA, Appel MJ.** 1996. A canine distemper virus epidemic in Serengeti lions (Panthera leo). Nature **379:**441–445. http://dx.doi.org/10.1038/379441a0.
4. **Domingo M, Ferrer L, Pumarola M, Marco A, Plana J, Kennedy S, McAliskey M, Rima BK.** 1990. Morbillivirus in dolphins. Nature **348:**21. http://dx.doi.org/10.1038/348021a0.
5. **Lamb RA, Parks GD.** 2007. Paramyxoviridae: the viruses and their replication, p 1449–1496. *In* Fields B, Knipe DM, Howley PM (ed), Fields virology, 5th ed. Lippincott Williams & Wilkins, Philadelphia, PA.
6. **Tatsuo H, Ono N, Tanaka K, Yanagi Y.** 2000. SLAM (CDw150) is a cellular receptor for measles virus. Nature **406:**893–897. http://dx.doi.org/10.1038/35022579.
7. **Muhlebach MD, Mateo M, Sinn PL, Prufer S, Uhlig KM, Leonard VH, Navaratnarajah CK, Frenzke M, Wong XX, Sawatsky B, Ramachandran S, McCray PB, Jr, Cichutek K, von Messling V, Lopez M, Cattaneo R.** 2011. Adherens junction protein nectin-4 is the epithelial receptor for measles virus. Nature **480:**530–533. http://dx.doi.org/10.1038/nature10639.
8. **Vongpunsawad S, Oezgun N, Braun W, Cattaneo R.** 2004. Selectively receptor-blind measles viruses: identification of residues necessary for SLAM- or CD46-induced fusion and their localization on a new hemagglutinin structural model. J Virol **78:**302–313. http://dx.doi.org/10.1128/JVI.78.1.302-313.2004.
9. **von Messling V, Oezguen N, Zheng Q, Vongpunsawad S, Braun W, Cattaneo R.** 2005. Nearby clusters of hemagglutinin residues sustain SLAM-dependent canine distemper virus entry in peripheral blood mononuclear cells. J Virol **79:**5857–5862. http://dx.doi.org/10.1128/JVI.79.9.5857-5862.2005.
10. **Langedijk JP, Janda J, Origgi FC, Orvell C, Vandevelde M, Zurbriggen A, Plattet P.** 2011. Canine distemper virus infects canine keratinocytes and immune cells by using overlapping and distinct regions located on one side of the attachment protein. J Virol **85:**11242–11254. http://dx.doi.org/10.1128/JVI.05340-11.
11. **Brindley MA, Takeda M, Plattet P, Plemper RK.** 2012. Triggering the measles virus membrane fusion machinery. Proc Natl Acad Sci U S A **109:**E3018–E3027. http://dx.doi.org/10.1073/pnas.1210925109.
12. **Ader N, Brindley MA, Avila M, Origgi FC, Langedijk JP, Orvell C, Vandevelde M, Zurbriggen A, Plemper RK, Plattet P.** 2012. Structural rearrangements of the central region of the morbillivirus attachment protein stalk domain trigger F protein refolding for membrane fusion. J Biol Chem **287:**16324–16334. http://dx.doi.org/10.1074/jbc.M112.342493.
13. **Navaratnarajah CK, Negi S, Braun W, Cattaneo R.** 2012. Membrane fusion triggering: three modules with different structure and function in the upper half of the measles virus attachment protein stalk. J Biol Chem **287:**38543–38551. http://dx.doi.org/10.1074/jbc.M112.410563.
14. **Ader N, Brindley M, Avila M, Orvell C, Horvat B, Hiltensperger G, Schneider-Schaulies J, Vandevelde M, Zurbriggen A, Plemper RK, Plattet P.** 2013. Mechanism for active membrane fusion triggering by morbillivirus attachment protein. J Virol **87:**314–326. http://dx.doi.org/10.1128/JVI.01826-12.
15. **Avila M, Alves L, Khosravi M, Ader-Ebert N, Origgi F, Schneider-Schaulies J, Zurbriggen A, Plemper RK, Plattet P.** 2014. Molecular determinants defining the triggering range of prefusion F complexes of canine distemper virus. J Virol **88:**2951–2966. http://dx.doi.org/10.1128/JVI.03123-13.
16. **Russell CJ, Jardetzky TS, Lamb RA.** 2001. Membrane fusion machines of paramyxoviruses: capture of intermediates of fusion. EMBO J **20:**4024–4034. http://dx.doi.org/10.1093/emboj/20.15.4024.
17. **Plemper RK, Hammond AL, Cattaneo R.** 2001. Measles virus envelope glycoproteins hetero-oligomerize in the endoplasmic reticulum. J Biol Chem **276:**44239–44246. http://dx.doi.org/10.1074/jbc.M105967200.
18. **Lee JK, Prussia A, Paal T, White LK, Snyder JP, Plemper RK.** 2008. Functional interaction between paramyxovirus fusion and attachment proteins. J Biol Chem **283:**16561–16572. http://dx.doi.org/10.1074/jbc.M801018200.
19. **Paal T, Brindley MA, St Clair C, Prussia A, Gaus D, Krumm SA, Snyder JP, Plemper RK.** 2009. Probing the spatial organization of measles virus fusion complexes. J Virol **83:**10480–10493. http://dx.doi.org/10.1128/JVI.01195-09.
20. **Apte-Sengupta S, Negi S, Leonard VH, Oezguen N, Navaratnarajah CK, Braun W, Cattaneo R.** 2012. Base of the measles virus fusion trimer head receives the signal that triggers membrane fusion. J Biol Chem **287:**33026–33035. http://dx.doi.org/10.1074/jbc.M112.373308.
21. **Bose S, Heath CM, Shah PA, Alayyoubi M, Jardetzky TS, Lamb RA.** 2013. Mutations in the parainfluenza virus 5 fusion protein reveal domains important for fusion triggering and metastability. J Virol **87:**13520–13531. http://dx.doi.org/10.1128/JVI.02123-13.
22. **Plattet P, Langedijk JP, Zipperle L, Vandevelde M, Orvell C, Zurbriggen A.** 2009. Conserved leucine residue in the head region of morbillivirus fusion protein regulates the large conformational change during fusion activity. Biochemistry **48:**9112–9121. http://dx.doi.org/10.1021/bi9008566.
23. **Plattet P, Plemper RK.** 2013. Envelope protein dynamics in paramyxovirus entry. mBio **4**(4):e00413-13. http://dx.doi.org/10.1128/mBio.00413-13.
24. **Jardetzky TS, Lamb RA.** 2014. Activation of paramyxovirus membrane fusion and virus entry. Curr Opin Virol **5:**24–33. http://dx.doi.org/10.1016/j.coviro.2014.01.005.
25. **Mateo M, Navaratnarajah CK, Cattaneo R.** 2014. Structural basis of efficient contagion: measles variations on a theme by parainfluenza viruses. Curr Opin Virol **5:**16–23. http://dx.doi.org/10.1016/j.coviro.2014.01.004.
26. **Palmer SG, Porotto M, Palermo LM, Cunha LF, Greengard O, Moscona A.** 2012. Adaptation of human parainfluenza virus to airway epithelium reveals fusion properties required for growth in host tissue. mBio **3**(3): e00137-12. http://dx.doi.org/10.1128/mBio.00137-12.
27. **Aguilar HC, Matreyek KA, Filone CM, Hashimi ST, Levroney EL, Negrete OA, Bertolotti-Ciarlet A, Choi DY, McHardy I, Fulcher JA, Su SV, Wolf MC, Kohatsu L, Baum LG, Lee B.** 2006. N-glycans on Nipah virus fusion protein protect against neutralization but reduce membrane fusion and viral entry. J Virol **80:**4878–4889. http://dx.doi.org/10.1128/JVI.80.10.4878-4889.2006.
28. **Bishop KA, Hickey AC, Khetawat D, Patch JR, Bossart KN, Zhu Z, Wang LF, Dimitrov DS, Broder CC.** 2008. Residues in the stalk domain of the Hendra virus G glycoprotein modulate conformational changes associated with receptor binding. J Virol **82:**11398–11409. http://dx.doi.org/10.1128/JVI.02654-07.
29. **Plemper RK, Hammond AL, Gerlier D, Fielding AK, Cattaneo R.** 2002. Strength of envelope protein interaction modulates cytopathicity of mea-

sles virus. J Virol **76:**5051–5061. http://dx.doi.org/10.1128/JVI.76.10.5051-5061.2002.
30. **Melanson VR, Iorio RM.** 2004. Amino acid substitutions in the F-specific domain in the stalk of the Newcastle disease virus HN protein modulate fusion and interfere with its interaction with the F protein. J Virol **78:**13053–13061. http://dx.doi.org/10.1128/JVI.78.23.13053-13061.2004.
31. **Iorio RM, Melanson VR, Mahon PJ.** 2009. Glycoprotein interactions in paramyxovirus fusion. Future Virol **4:**335–351. http://dx.doi.org/10.2217/fvl.09.17.
32. **Iorio RM, Mahon PJ.** 2008. Paramyxoviruses: different receptors—different mechanisms of fusion. Trends Microbiol **16:**135–137. http://dx.doi.org/10.1016/j.tim.2008.01.006.
33. **Hashiguchi T, Ose T, Kubota M, Maita N, Kamishikiryo J, Maenaka K, Yanagi Y.** 2011. Structure of the measles virus hemagglutinin bound to its cellular receptor SLAM. Nat Struct Mol Biol **18:**135–141. http://dx.doi.org/10.1038/nsmb.1969.
34. **Welch BD, Yuan P, Bose S, Kors CA, Lamb RA, Jardetzky TS.** 2013. Structure of the parainfluenza virus 5 (PIV5) hemagglutinin-neuraminidase (HN) ectodomain. PLoS Pathog **9:**e1003534. http://dx.doi.org/10.1371/journal.ppat.1003534.
35. **Yuan P, Swanson KA, Leser GP, Paterson RG, Lamb RA, Jardetzky TS.** 2011. Structure of the Newcastle disease virus hemagglutinin-neuraminidase (HN) ectodomain reveals a four-helix bundle stalk. Proc Natl Acad Sci U S A **108:**14920–14925. http://dx.doi.org/10.1073/pnas.1111691108.
36. **Bose S, Song AS, Jardetzky TS, Lamb RA.** 2014. Fusion activation through attachment protein stalk domains indicates a conserved core mechanism of paramyxovirus entry into cells. J Virol **88:**3925–3941. http://dx.doi.org/10.1128/JVI.03741-13.
37. **Liu Q, Stone JA, Bradel-Tretheway B, Dabundo J, avides Montano JA, Santos-Montanez J, Biering SB, Nicola AV, Iorio RM, Lu X, Aguilar HC.** 2013. Unraveling a three-step spatiotemporal mechanism of triggering of receptor-induced Nipah virus fusion and cell entry. PLoS Pathog **9:**e1003770. http://dx.doi.org/10.1371/journal.ppat.1003770.
38. **Apte-Sengupta S, Navaratnarajah CK, Cattaneo R.** 2013. Hydrophobic and charged residues in the central segment of the measles virus hemagglutinin stalk mediate transmission of the fusion-triggering signal. J Virol **87:**10401–10404. http://dx.doi.org/10.1128/JVI.01547-13.
39. **Brindley MA, Suter R, Schestak I, Kiss G, Wright ER, Plemper RK.** 2013. A stabilized headless measles virus attachment protein stalk efficiently triggers membrane fusion. J Virol **87:**11693–11703. http://dx.doi.org/10.1128/JVI.01945-13.
40. **Orvell C, Sheshberadaran H, Norrby E.** 1985. Preparation and characterization of monoclonal antibodies directed against four structural components of canine distemper virus. J Gen Virol **66:**443–456. http://dx.doi.org/10.1099/0022-1317-66-3-443.
41. **Cherpillod P, Beck K, Zurbriggen A, Wittek R.** 1999. Sequence analysis and expression of the attachment and fusion proteins of canine distemper virus wild-type strain A75/17. J Virol **73:**2263–2269.